

# Analyzing a Deformable Model Using Differential Geometry

PAULO F. DE SANTA CLARA RAMOS JR.<sup>1</sup>, WU, SHIN -TING<sup>1</sup>, SUELI I. R. COSTA<sup>2</sup>

<sup>1</sup> Faculdade de Engenharia Elétrica e de Computação

Universidade Estadual de Campinas

C.P. 6101 - Campinas - São Paulo - Brazil

{pauloscr,ting}@dca.fee.unicamp.br

<sup>2</sup> Instituto de Matemática

Universidade Estadual de Campinas

sueli@ime.unicamp.br

**Abstract.** This paper explores the use of elements of Differential Geometry to control the manipulation of the deformable model proposed by Terzopoulos et al. [8] for animating deformable objects. Particularly, we are interested on the animation of deformable panels without stretching (area invariant), such as clothes and papers. Based on our analysis we could generate with a little effort several simulations compatible with our expectation.

## 1 Introduction

The deformable model proposed by Terzopoulos et al. [8] is founded on the motion equation in Lagrangean form and adjust the elastic deformation by parameters related to the metric and curvature tensors of surfaces. Since it unifies the description of shape and motion, this model significantly simplifies the approach of animating complex objects.

The flexibility and the modeling power of this model is recognized by the modeling community. Several subsequent works [4, 2, 6] were made to improve this approach. A major problem, which was not enough discussed, is how to manipulate the parameters to get realistic dynamics behavior.

This work addresses this problem. Using concepts from Differential Geometry, we take advantage of the geometric potential of the model and deal more intuitively with parameters in order to get realistic simulation or physical movements through an intuitive interface.

A major challenge that we faced was the non-independency between these parameters. This interdependency, which is a consequence of the differential relation between the metric and the curvature tensors, has not been considered up to now, and, as we could see, non-compatible parameters can yield non-realistic deformations.

In our analysis we deal more specifically with the class of surfaces with a big resistance against stretching and little resistance against curvature. These features would allow us to simulate the behavior of a great variety of physical objects, like a piece of cloth or a sheet of paper.

This article is organized as follows. In section 2

some basic concepts from Differential Geometry and a brief description of the analyzed model are given. We discuss in section 3 the geometric meaning of the model parameters and their influence on the visual effects. The adjustment of the elasticity parameters is shown in section 4. Some simulation results are given in section 5. Finally, in section 6 some concluding remarks are drawn.

## 2 Deformable Model

To be self-contained a brief description of the analyzed deformable model is given.

### 2.1 Basic Concepts

For the vector position  $\vec{r}(x, y, z)$  of a point  $P$  in a 3-dimensional Euclidean space, we can associate its coordinates to a unique set of coordinates  $(a_1, \dots, a_n)$ :

$$\begin{aligned}x &= x(a_1, \dots, a_n) \\y &= y(a_1, \dots, a_n) \\z &= z(a_1, \dots, a_n)\end{aligned}\tag{1}$$

The coordinates  $(a_1, \dots, a_n)$  are known as *curvilinear coordinates* of  $P$ . The value of  $n$  is related to the dimension of the object in 3D space to which the point belongs. For  $n = 1$  the object is a curve, for  $n = 2$ , a surface, and  $n = 3$ , a solid body.

Since we have

$$d\vec{r} = \frac{\partial \vec{r}}{\partial a_1} da_1 + \dots + \frac{\partial \vec{r}}{\partial a_n} da_n,\tag{2}$$

the squared length of an arc in curvilinear coordinates can be expressed by

$$dl^2 = d\vec{r} \cdot d\vec{r} = \sum_i^n \sum_j^n G_{ij} da_i da_j, \quad (3)$$

where

$$G_{ij}(\vec{r}(\vec{a})) = \frac{\partial \vec{r}}{\partial a_i} \cdot \frac{\partial \vec{r}}{\partial a_j}. \quad (4)$$

Equation (3) is known as *first fundamental form* or *metric tensor* and the elements  $G_{ij}$  are called *metric coefficients* [1, 7, 3].

In this paper, we shall also use the notation  $A_b$  to designate the partial derivative  $\frac{\partial A}{\partial b}$ . That is, equation (4) can be rewritten as

$$G_{ij}(\vec{r}(\vec{a})) = \vec{r}_{a_i} \cdot \vec{r}_{a_j}. \quad (5)$$

The *curvature* of a curve at a given point measures the amount of variation of the unitary tangent vector to that point from its neighborhood (angle variation). The *normal curvature* of a point  $P$  that lays on a curve  $C$  of a surface  $S$  is given by:

$$k_n = k \cos \theta, \quad (6)$$

where  $k$  is the curvature of  $C$  in  $P$  and  $\theta$  is the angle between the principal normal to  $C$  and the normal vector to  $S$ , in  $P$  [1, 7, 3].

It can be shown that

$$k_n = \sum_i^2 \sum_j^2 B_{ij} da_i da_j, \quad (7)$$

where

$$B_{ij}(\vec{r}(\vec{a})) = \vec{n} \cdot \frac{\partial^2 \vec{r}}{\partial a_i \partial a_j} = \vec{n} \cdot \vec{r}_{a_i a_j}. \quad (8)$$

Equation (7) is called *second fundamental form* or *curvature tensor* and the elements  $B_{ij}$  are said *curvature coefficients*.

Roughly speaking, the coefficients  $G_{ij}$  of the first fundamental form are related to the length and area measures or stretching of a surface (metric tensor) whereas the second fundamental form  $B_{ij}$  describes the bending or how non-planar is a surface (curvature tensor).

The values of  $B_{ij}$  can be obtained from  $G_{ij}$  according to the following relations:

$$B_{11} = \frac{\left\| \begin{array}{ccc} x_{a_1 a_1} & y_{a_1 a_1} & z_{a_1 a_1} \\ x_{a_1} & y_{a_1} & z_{a_1} \\ x_{a_2} & y_{a_2} & z_{a_2} \end{array} \right\|}{\sqrt{G_{11}G_{22} - G_{12}^2}}$$

$$B_{12} = B_{21} = \frac{\left\| \begin{array}{ccc} x_{a_1 a_2} & y_{a_1 a_2} & z_{a_1 a_2} \\ x_{a_1} & y_{a_1} & z_{a_1} \\ x_{a_2} & y_{a_2} & z_{a_2} \end{array} \right\|}{\sqrt{G_{11}G_{22} - G_{12}^2}}$$

$$B_{22} = \frac{\left\| \begin{array}{ccc} x_{a_2 a_2} & y_{a_2 a_2} & z_{a_2 a_2} \\ x_{a_1} & y_{a_1} & z_{a_1} \\ x_{a_2} & y_{a_2} & z_{a_2} \end{array} \right\|}{\sqrt{G_{11}G_{22} - G_{12}^2}} \quad (9)$$

The metric and the curvature tensors are then not independent, they must satisfy certain compatibility differential equations known as Gauss formula and Mainardi-Codazzi equations from surface theory. These equations are deduced from the relations

$$\begin{aligned} (\vec{r}_{a_1 a_1})_{a_2} - (\vec{r}_{a_1 a_2})_{a_1} &= \vec{0} \\ (\vec{r}_{a_2 a_2})_{a_1} - (\vec{r}_{a_2 a_1})_{a_2} &= \vec{0} \\ \vec{N}_{a_1 a_2} - \vec{N}_{a_2 a_1} &= \vec{0} \end{aligned} \quad (10)$$

On the other hand, two symmetric tensors  $G_{ij}$  and  $B_{ij}$ , with  $G_{11} > 0$ ,  $G_{22} > 0$  and  $\det G > 0$ , satisfying those compatibility conditions determine up to a rigid motion a unique surface which has  $G_{ij}$  and  $B_{ij}$  for metric and curvature tensors [1, 7, 3].

## 2.2 A Deformable Model

Our deformable surfaces follow the implementation of a physically-based model and their dynamics are ruled by the equation of motion in its Lagrangean formulation:

$$\mu \frac{\partial^2 \vec{r}}{\partial t^2} + \gamma \frac{\partial \vec{r}}{\partial t} + \frac{\delta \varepsilon(\vec{r})}{\delta \vec{r}} = \vec{f}(\vec{r}, t). \quad (11)$$

In equation (11),  $\mu$  is the mass density and  $\gamma$  is the dumping constant at a point  $\vec{r}$ . The vector  $\vec{f}$  denotes the total contribution of external forces at  $\vec{r}$  in an instant  $t$ . The term corresponding to the internal energies accumulated due to elastical deformation  $\varepsilon(\vec{r})$  is estimated from the following empirical consideration [8]:

$$\varepsilon(\vec{r}) = \int_{\Omega} (\|\mathbf{G} - \mathbf{G}^0\|_{\alpha}^2 + \|\mathbf{B} - \mathbf{B}^0\|_{\beta}^2) da_1 da_2, \quad (12)$$

which takes, for the metric and curvature tensors, a weighted norm of the difference between the deformed state and rest state values. That measure can *reasonably* estimate the elastical energy of a surface, attaching the amount of energy to the variations in the surface's geometric shape. In other words, that norm is a measure of the energy needed to displace the surface's points, defined over a region  $\Omega$ , from their rest state.

Applying the weighted norms of equation (12), we obtain the following simplified deformation energy:

$$\varepsilon(\vec{\mathbf{r}}) = \int_{\Omega} \sum_{i,j} (\eta_{ij} (G_{ij} - G_{ij}^0)^2 + \xi_{ij} (B_{ij} - B_{ij}^0)^2) da_1 da_2 \quad (13)$$

The weights  $\eta_{ij}$  and  $\xi_{ij}$  are denominated elasticity parameters.

From equation (12) we may have a good approximation for the internal force  $\delta\varepsilon(\vec{\mathbf{r}})/\delta\vec{\mathbf{r}}$  due to deformations on the object [6]:

$$\vec{\mathbf{e}}(\vec{\mathbf{r}}) = \sum_{i,j} -\frac{\partial}{\partial a_i} \cdot \left( \alpha_{ij} \frac{\partial \vec{\mathbf{r}}}{\partial a_j} \right) + \frac{\partial^2}{\partial a_i \partial a_j} \left( \beta_{ij} \frac{\partial^2 \vec{\mathbf{r}}}{\partial a_i \partial a_j} \right), \quad (14)$$

where the variables  $\alpha_{ij}$  and  $\beta_{ij}$  are defined as:

$$\begin{aligned} \alpha_{ij}(\vec{\mathbf{a}}, \vec{\mathbf{r}}) &= \eta_{ij}(\vec{\mathbf{a}})(G_{ij} - G_{ij}^0) \\ \beta_{ij}(\vec{\mathbf{a}}, \vec{\mathbf{r}}) &= \xi_{ij}(\vec{\mathbf{a}})(B_{ij} - B_{ij}^0). \end{aligned} \quad (15)$$

Since the quantities  $G_{ij}$  are related to surface stretching, while the values for  $B_{ij}$  are related to curvature, our measures of deformation follow from these quantities and the surface's behavior of resistance to external forces will be as much effective as greater are the values assigned to the elasticity parameters.

### 2.3 Discretization

We make a discretization of equation (14) with finite difference techniques, according to the suggestion of Terzopoulos [8]. The discretization turns the partial differential equation into a linear system of differential equations.

The continuous space  $\Omega$  is then discretized into a MxN-node mesh, where each node  $(m, n)$  represents a discrete point (or a *nodal variable*)  $\vec{\mathbf{r}}(m, n)$  in 3D space. To the set of nodal variables  $\vec{\mathbf{r}}(m, n)$  defined for MxN nodes we call *function mesh* and each node is referred to as  $\vec{\mathbf{r}}[m, n]$ .

Denoting  $D^+$  the first-order forward finite difference and  $D^-$  the first-order backward finite difference, equations (14) and (15) are respectively discretized into

$$e_{ij}[m, n] = \sum_{i,j}^2 -D_i^- (\vec{\mathbf{p}})[m, n] + D_{ij}^{(-)} (\vec{\mathbf{q}})[m, n] \quad (16)$$

where

$$\begin{aligned} \vec{\mathbf{p}} &= \alpha_{ij}[m, n] D_j^+ (\vec{\mathbf{r}})[m, n] \\ \vec{\mathbf{q}} &= \beta_{ij}[m, n] D_{ij}^{(+)} (\vec{\mathbf{r}})[m, n] \end{aligned} \quad (17)$$

and

$$\alpha_{ij}[m, n] = \eta_{ij}[m, n] (D_i^+ (\vec{\mathbf{r}})[m, n] \cdot D_j^+ (\vec{\mathbf{r}})[m, n] - G_{ij}^0) \quad (18)$$

$$\beta_{ij}[m, n] = \xi_{ij}[m, n] (\vec{\mathbf{u}}[m, n] \cdot D_{ij}^{(+)} (\vec{\mathbf{r}})[m, n] - B_{ij}^0). \quad (19)$$

One can observe that the values for the difference operators are not determined for points laying at the boundaries of domain  $\Omega$ . Nevertheless, a natural condition of boundary can be simulated by assigning a *zero* value to any difference operator of equation (17) that refers to points  $\vec{\mathbf{r}}(m, n)$  not belonging to the set of MxN points of our mesh.

If the nodal variables in function meshes  $\mathbf{r}[m, n]$  and  $\mathbf{e}[m, n]$  are grouped, respectively, into column matrices  $\mathcal{R}$  and  $\mathcal{E}$  of dimension MxN, then equation (16) can be written in matrix form

$$\mathcal{E} = \mathbf{K}(\vec{\mathbf{r}})\mathcal{R} \quad (20)$$

where  $\mathbf{K}$  is known as *strength matrix*.

The discrete form of the equation of motion can then be expressed by the following coupled system of differential equations:

$$\mathbf{M} \frac{\partial^2 \vec{\mathcal{R}}}{\partial t^2} + \mathbf{C} \frac{\partial \vec{\mathcal{R}}}{\partial t} + \mathbf{K}(\vec{\mathbf{r}})\mathcal{R} = \mathcal{F} \quad (21)$$

where

- $\mathbf{M}$  is the diagonal matrix formed by the mass density of each element,
- $\mathbf{C}$ , the diagonal matrix formed by the dumping density of each element, and
- $\mathcal{F}$ , the column matrix containing the external force applied to each element, calculated from  $\vec{\mathbf{f}}(\vec{\mathbf{r}}, t)$ .

To simulate the dynamics of a non-rigid object, the system of differential equations (21) must be integrated through time. Those equations will be integrated using a step-by-step process, which now converts a system of non-linear differential equations into a sequence of linear systems.

The time interval from  $t=0$  to  $t=T$  is subdivided into smaller time intervals of same duration  $\Delta t$  and the integration process carries out the calculations for the sequence of approximated solutions for instants  $t, t+\Delta t, t+2\Delta t, \dots, T$ . Computing  $\mathcal{E}$  in  $t+\Delta t$  and  $\mathcal{F}$  in  $t$ , and substituting the discrete-time approximations

$$\frac{\partial^2 \mathcal{R}}{\partial t^2} = (\mathcal{R}_{t+\Delta t} - 2\mathcal{R} + \mathcal{R}_{t-\Delta t})/\Delta t^2 \quad (22)$$

$$\frac{\partial \mathcal{R}}{\partial t} = (\mathcal{R}_{t+\Delta t} - \mathcal{R}_{t-\Delta t})/2\Delta t \quad (23)$$

in equation (21), we obtain

$$\mathbf{A}_t \mathcal{R}_{t+\Delta t} = \mathcal{G}, \quad (24)$$

where

$$\mathbf{A}_t = \mathbf{K}(\vec{\mathbf{r}}_t) + \left( \frac{1}{\Delta t^2} \mathbf{M} + \frac{1}{2\Delta t} \mathbf{C} \right) \quad (25)$$

and

$$\mathcal{G}_t = \mathcal{F}_t + \left( \frac{1}{\Delta t^2} \mathbf{M} + \frac{1}{2\Delta t} \mathbf{C} \right) \mathcal{R}_t + \left( \frac{1}{\Delta t} \mathbf{M} - \frac{1}{2} \mathbf{C} \right) \mathcal{V}_t. \quad (26)$$

The column matrix of speed  $\mathcal{V}_t$  is given by:

$$\mathcal{V}_t = (\mathcal{R}_t - \mathcal{R}_{t-\Delta t})/\Delta t. \quad (27)$$

### 3 Control

Observing equations (11) and (12) we will see that the geometric shape of a deformable surface can be controlled not only by  $\mu$ ,  $\gamma$  and external forces  $\vec{\mathbf{f}}(\vec{\mathbf{r}}, t)$ , but also by the elasticity parameters. Due to the diversity of parameters involved, different combinations of those parameters could take us to the same visual effect.

For example, to generate the animation of an oscillating surface, we can apply sinusoidal forces to each point of the surface, or we can assign distinct values of  $\gamma$  to each point, or, alternatively, assign different values to  $\mu$  in each point, or we can even define convenient values for the elasticity parameters.

That flexibility increases the model's versatility, but, on the other hand, makes it difficult to be controlled, since these parameters are not orthogonal and the influence of some parameter value can be masked by another's.

The procedure we propose tries to overcome this trade-off by assigning to each parameter a dominant independent rule in such a way that all possible value combinations could generate the set of all desirable visual effects. Besides that, according to the tools required to analyze the influence of those parameters, we make a distinction of two control levels:

**Macro-control:** By assigning adequate values for  $\mu$ ,  $\gamma$  and  $\vec{\mathbf{f}}$ , we may have an inaccurate, but intuitive control of the object's dynamics. All points in the surface assume equal values of  $\mu$  and  $\gamma$ , considering that the surface is homogeneous with respect to the environment in which it is immersed.

**Micro-control:** The variations in the local geometry of each point are caused by the material's resistance to variations in stretching and curving. That effect can be controlled by properly setting the elasticity parameters  $\eta_{ij}$  and  $\xi_{ij}$ .

### 3.1 Macro Control

As equation (11) refers to each surface point at its position  $\vec{\mathbf{r}}(a_1, a_2)$ , we can analyze that equation's influence by taking into account the similarities with a mass-coil system at each of those points. In that way, if the value assigned to  $\gamma$  is too large in comparison with the value assigned to  $\mu$ , each point will have a over-damped behavior. Thus, the surface would reach an equilibrium state more quickly. As we increase the value assigned to  $\mu$ , the surface tends to respond to perturbations in an oscillating manner before equilibrium is reached, owe to the increased inertia (damped oscillation). Finally, when  $\gamma$  is null, the surface keeps oscillating around an equilibrium point.

In accordance to what has been already observed by Thalmann *et al.* [2], in real situations the value for  $\gamma$  must be a function that takes into account the dissipative effects coming from internal frictions in the surface. They have proposed a model that calculates the dumping contribution also as a function of the metric and curvature tensors. Nevertheless, for the class of objects we have been studying, we have realized that some very realistic results can be obtained considering  $\gamma$  as a scalar and just adjusting the values of  $\mu$  and  $\vec{\mathbf{f}}$ .

In addition to that, we have observed that the triples  $(a\mu, b\gamma, c\vec{\mathbf{f}})$ , where  $a, b, c > 0$ , produce the same visual effect, since substituting them into equation (11) we obtain a set of equivalent equations that generate the same  $\vec{\mathbf{r}}$  at each iteration. This is an important observation from the numeric point of view, in the sense that it is always possible to "scale" the equations to a computationally more feasible range of values.

By now, it should be emphasized that the idea of increasing the values of physical parameters is not merely a change in scale. Our procedure corresponds to trying new combinations of macro-control parameters, but the description assigned to the object's rest-state size should be maintained. If the object's size was increased likewise, we would incur in the same values of nodal variables and no dynamic changes would be noticed.

### 3.2 Micro Control

According to Terzopoulos [8], there are two ways of adjusting the amount of deformability of a surface. It can be done by setting parameters  $\eta_{ij}$  and  $\xi_{ij}$  or by setting parameters  $\alpha_{ij}$  and  $\beta_{ij}$ .

The parameters  $\eta_{ij}$  and  $\xi_{ij}$  are weights of quadratic terms (equation (13)). When the variations in the object's geometry,  $G_{ij}$  and  $B_{ij}$ , with respect to

its rest state shape,  $G_{ij}^0$  and  $B_{ij}^0$ , are very large or very small, the observed results may be very critical, depending on the values assigned to  $\eta_{ij}$  and  $\xi_{ij}$ . Under the numerical point of view, we are working with non-linear systems, which are more susceptible to run into instability.

If we take a careful look into the equations (14) and (15), we may conclude that non-realistic behaviors are more likely to happen when we work directly manipulating parameters  $\alpha_{ij}$  and  $\beta_{ij}$ . That stems from the fact that positive values assigned directly to  $\alpha_{ij}$  and  $\beta_{ij}$  always induce a residual initial elastic energy. That situation would be equivalent to having  $(G_{ij} - G_{ij}^0)$ , as well as  $(B_{ij} - B_{ij}^0)$ , non-zero even when the external force  $\vec{f}$  is absent and no change in geometry is produced.

To avoid that inconsistency, we take the approach of using parameters  $\eta_{ij}$  and  $\xi_{ij}$  to control elasticity in our simulations, as they act directly upon the variations of the metric and curvature tensors.

It is worth to mention that the empirical choice of values for  $\eta_{ij}$  and  $\xi_{ij}$  must be quite criterious. According to equations (15), when the values of  $\eta_{ij}$  and  $\xi_{ij}$  are set too large, exaggerated contributions of the restoring elastic force occur and these contributions lead our dynamic system to a loss of equilibrium. That comes from the fact that the internal energy is calculated as a function of  $\alpha_{ij}$  and  $\beta_{ij}$  (equation (12)). Exaggerated values of  $\eta_{ij}$  and  $\xi_{ij}$  may produce large values of  $\alpha_{ij}$  and  $\beta_{ij}$  even for slight tensor variations.

To have a better understanding of the influence of parameters  $\eta_{ij}$  and  $\xi_{ij}$  in the visual effects, it is interesting to examine, from the geometric point of view, the meaning of the variations in parameters  $G_{ij}$  and  $B_{ij}$ , as well as the relations between these variations. As it has been mentioned before, the variations in  $G_{ij}$  are related to area variations while variations in  $B_{ij}$  reflect changes in mean curvature.

One can intuitively see that these tensor variations are attached to each other if we consider the case of a plane surface with its border held fixed (Fig. 1). In this case, it would be impossible to stretch the surface (*i.e.*: increase its area) without producing curvature effects (Fig. 2). There must be coherence between stretching and bending. This coherence is stated by the equations (10). Based on these equations, we derived a compatibility test which compares the involved vectors through the ratio of its magnitudes and the cosine of its angles (both numbers must be near to one).

So, as  $\eta_{ij}$  and  $\xi_{ij}$  weight those variations, we can predict that our model may be driven to instability if we increase the value of  $\xi_{ij}$  while maintaining  $\eta_{ij}$

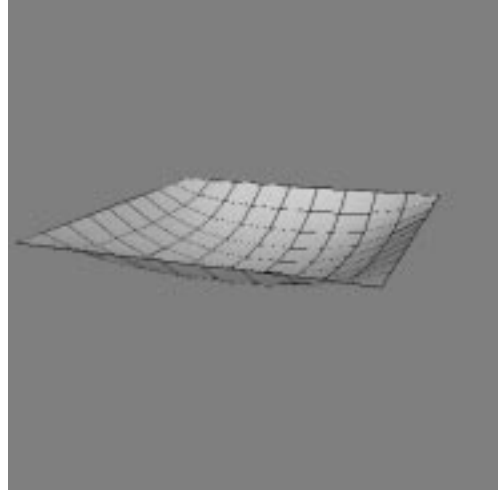


Figure 1: A panel resistant to stretching.

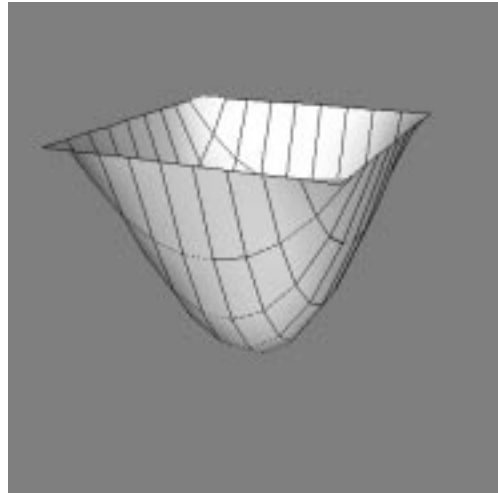


Figure 2: Same panel of Fig. 1 with decreased stretching resistance

relatively small. Depending on the configuration of external forces and boundary conditions, that is, the restrictions we apply to our deformable surface, that instability can be reached quite easily.

A relevant point which should be discussed now is the accuracy of the surface discretization process, as the numerical method used to solve our system relies strongly on that. From equations (16), (18) and (19) it is easy to verify that the calculated values for  $G_{ij}$  and  $B_{ij}$  may present errors generated by the finite difference technique. Those errors can produce unexpected results. On the other hand, a more refined discretization considerably increases the number of points in the mesh, making the solution a time-consuming process. Due to our interest in interactive solutions, which would return to the user

non-ambiguous results as quickly as possible, we decided for rather raw discretizations.

From equations (15) we may notice that parameters  $\eta_{ij}$  and  $\xi_{ij}$  may be used to mask some errors produced by the discretization process. Although the proposed model does not present any restriction nor any direct control upon the coordinate system  $(a_1, a_2)$  to be used, it is recommended to work with orthogonal systems and perform some suitable simplifications in the calculations. A reasonable simplification for the algorithm presented in section 2.3 consists of making, for each iteration,  $\alpha_{12} = \alpha_{21} = \beta_{12} = \beta_{21} = 0$  for all points in the surface, so that there would be no contribution from these quantities to the evaluation of deformation energy  $\varepsilon(\vec{r})$ . This can be achieved by letting  $\eta_{12} = \eta_{21} = \xi_{12} = \xi_{21} = 0$  and we have adopted such procedure in all of our simulations.

In addition to that, as we have been proposing some way of modeling flexible objects with no variations in area, we theoretically expect successful simulations using large values for  $\eta_{ij}$  and small ones for  $\xi_{ij}$ . As it is stated in equation (12), the weighting factors  $\eta_{ij}$  would therefore have more influence on the evaluation of internal energy than the weighting factors  $\xi_{ij}$ .

#### 4 The Choice of Parameter Values

Examining the combinations of values assigned to the most satisfactory results achieved up to now (some of which are listed in section 5), we notice that the values for  $\eta_{ij}$  and  $\xi_{ij}$  are much smaller than that of the rest of the physical parameters involved. As we are working with finite precision, the useful range of values for  $\eta_{ij}$  and  $\xi_{ij}$  may become so restricted that practically no noticeable change in visual effects will occur as influence of these parameters.

In general, due to equation (12), if the other physical parameters are set to a range of values similar to the one found in real world, then great values assigned to  $\eta_{ij}$  or  $\xi_{ij}$  would result in instability and, in contrast to this, smaller values may not produce substantial changes in the surface's dynamic behavior.

One way of overcoming this problem is to increase the values of all physical parameters involved, as mentioned in section 3.1. Doing this, we can increase the upper bound (imposed by instability) for  $\eta_{ij}$  and  $\xi_{ij}$ , allowing variations of these two parameters within a broader range. As a consequence of that, we can obtain a richer set of realistic effects in our simulations.

When increasing the values of our parameters to reach an adequate range for performing computa-

tions, we may come to a situation where the values have little intuitive meaning as they may be considerably different from the ones we find in real world. So we have to figure out some way of preserving the intuitive character, which is an important feature of physically-based modeling, for the sake of controllability.

A possible solution for maintaining the intuitive aspect of our model would be to set, at first, the values for our physical parameters based on the values we find in real world, according to the measuring system we are used to (in our case, we choose the International System, also known as MKS). From that initial intuitive approximation we carry out our transformations of multiplying them by constants to make them more suitable for numerical calculations. At last, we do the fine adjustments related to the dynamics of deformation with the elasticity parameters  $\eta_{ij}$  and  $\xi_{ij}$ . Using our terminology, those fine adjustments on stretching and curvature resistance are what we called micro-controlling.

#### 5 Simulation Examples

In this section, we present some simulation examples to illustrate and comment a few aspects related to the combinations of parameter values discussed so far. In all of our simulations we used  $\eta_{11} = \eta_{22} = \eta$  and  $\xi_{11} = \xi_{22} = \xi$ .

Our first example involves the simulation of an opening curtain. The physical parameters  $\mu$ ,  $\gamma$  and  $\vec{f}$  and the curtain dimensions are set to values based on real world. By applying external forces to the upper part of the curtain, perpendicular to the plane defined by its rest state and restricting its movement to the axis where it should slide, we achieve the effect seen in Figs. 3 to 6.

The parameter  $\xi$  is set to *zero* and the value assigned to  $\eta$  is reasonably high, in a way that the surface seems to fold with no resistance, however, suffering little stretching due to the external forces applied. It is important to say that, for such a combination of values, different values of  $\xi$  ranging from 0 to  $10^{-3}$  would not affect the surface's dynamic behavior, while for  $\xi > 10^{-3}$  we are led to instability.

By increasing the values of physical parameters  $\mu$ ,  $\gamma$  and  $\vec{f}$  we can experience more effective responses from  $\eta$  and  $\xi$ , as illustrated in the next pictures. Fig. 5 shows our curtain with a similar combination of elasticity parameters ( $\xi = 0$  and  $\eta$  large), but using higher values of  $\mu$ ,  $\gamma$  and  $\vec{f}$ .

In Fig. 6 we used the same combination of parameters as the one from the previous example, except that curvature resistance  $\xi$  is increased from 0 to  $3.0 \times 10^{-6}$ . In this example we can observe the



Figure 3: Opening curtain.

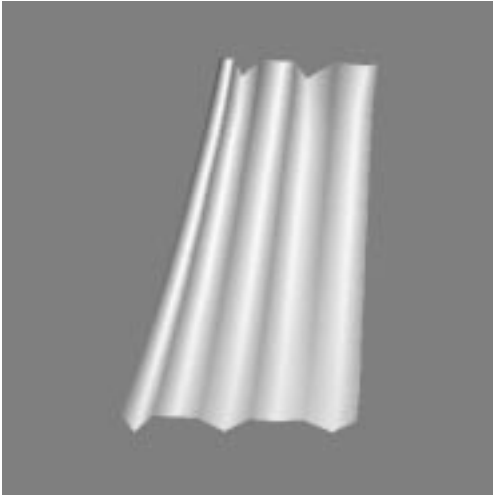


Figure 4: Same curtain of Fig. 3 after some elapsed time.

sensitivity achieved for  $\xi$  when the other parameter values are properly set.

Another way of checking the little resistance to curvature in contrast to the remarkable resistance to stretching is examining the simulation of an oscillating flag. In this case to simulate a wind behavior acting on a flag, we apply on one side of the flag a coil force. This force is responsible for the waving character of the resulted images presented in Figs. 7 and 8.

## 6 Conclusions

We have presented some results of an analysis of the deformable model proposed in [8] with the use of concepts from Differential Geometry. Differing from



Figure 5: “Scaled” parameters allow a simulation of light, silky behavior of a curtain.

other approaches to physically-based modeling, this model expresses the potential elastic energy in terms of metric and curvature tensors. Our goal has been to explore the geometric potential of this model and to devise a more intuitive interface for physically-based modeling.

We distinguished two control levels in the analyzed model: the level that simulates the motion of the object (macro-control) and the level that governs the shape deformation (micro-control). This leads to two functionally independent sets of parameters:  $\{\mu, \gamma, \vec{f}\}$  and  $\{\eta_{ij}, \xi_{ij}\}$ .

Since our interest was on the geometric aspect, we focused our discussion on the micro-control. We showed that, although  $G_{ij}$  and  $B_{ij}$  are non-independent, it is possible to include a compatibility test to ensure realistic visual effects in the simulations. In addition, we discussed how to choose  $\eta_{ij}$  and  $\xi_{ij}$  to get different variations on the shape deformation.

Although we have limited our study to the class of deformable but non-stretching (invariant area) surfaces, we believe that the methodology we proposed is suitable for any other case.

## 7 Acknowledgements

The pictures presented in this paper were rendered using X-Geomview 1.5.

## References

- [1] Berger, M. and Gostiaux, B.. *Differential Geometry: Manifolds, Curves, and Surfaces*. Springer-Verlag, New York, 1988.



Figure 6: Curvature resistance is increased to simulate paper behavior.

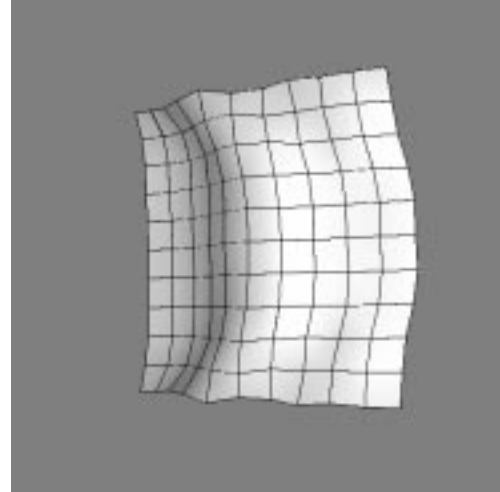


Figure 8: Same flag of Fig. 7 after some elapsed time.

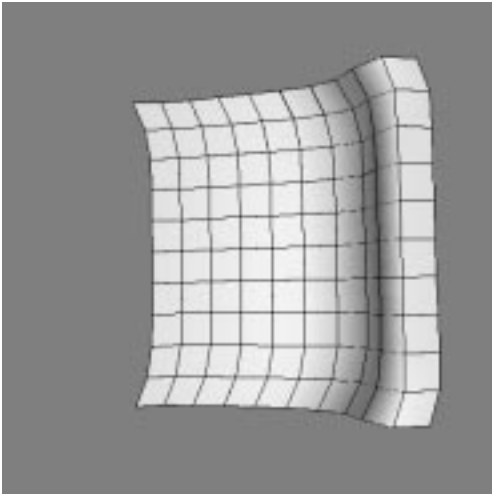


Figure 7: A waving flag.

- [2] Carignan, M., Yang Y., Thalmann, N. M., and Thalmann D.. *Dressing Animated Synthetic Actors with Complex Deformable Clothes*. Computer Graphics, 1992, Vol.26, No.2, pp.99-104.
- [3] Carmo, M.P.. *Differential Geometry of Curves and Surfaces*. Prentice Hall Englewood Cliffs, N.J., 1976.
- [4] Celniker, G. and Grossard, D.. *Deformable Curve and Surface Finite-elements for Free-form Shape Design*. Computer Graphics, 25(4):257-266, July 1991.
- [5] Feyman, C.R.. *Modelling the Appearance of Cloth*. MSc Thesis, Department of Electri-

cal Engineering and Computer Science, MIT, Cambridge, MA, 1986.

- [6] Horta, A.A. and Wu, S.T.. *Deformação de Superfícies Não Rígidas Baseada em Princípios Físicos*. Anais do VIII SIBGRAPI, 1995, pp.175-182.
- [7] Struik, D.J.. *Lectures on Classical Differential Geometry*. Addison-Wesley Publishing Co., London, 1961.
- [8] Terzopoulos, D., Platt J., Barr A., and Fleischer K.. *Elastically Deformable Models*. SIGGRAPH'87, Computer Graphics, 1987, Vol.21, No.4, pp.205-214.
- [9] Weil, J.. *The synthesis of cloth objects*. Computer Graphics, 1986, Vol.20, No.4, pp.49-54.